UNIVERSITY OF CALIFORNIA

Santa Barbara

Organic Semiconducting Molecules in Green Solvents

A Thesis submitted in partial satisfaction of the

requirements for the degree Master of Science

in Chemistry

by

Xiaofen Chen

Committee in charge:

Professor Guillermo C. Bazan, Chair

Professor Steven K. Buratto

Professor Thuc-Quyen Nguyen

Professor Javier Read de Alaniz

March 2015

The thesis of Xiaofen Chen is approved.

Steven K. Buratto

Thuc-Quyen Nguyen

Javier Read de Alaniz

Guillermo C. Bazan, Committee Chair

February 2015

Organic Semiconducting Molecules in Green Solvents

ACKNOWLEDGEMENTS

The work described herein would not be possible without the support and inspiration provided by family, friends, educators and co-workers over two years. I am lucky to have the opportunity to work as a junior specialist in Center of Polymer and Solids from 03/2011 to 09/2012, supervised by Professor Guillermo C. Bazan, who then encouraged me to pursue a PhD degree in Chemistry and Biochemistry department after one year. I do owe a very big thank you to Professor Gui. Bazan, for all the support and encouragement he afforded to me during my stay at UCSB. Collaborators in the Bazan and Nguyen research groups have provided useful information and stimulating discussion along the way. It is a great pleasure to interact with all the group members over many years. Additionally, the research and administrative staff in the Department of Chemistry and Biochemistry, the MRL and CNSI facilities have also provide supports that make my research and life in UCSB much easier. Finally I would like to thank my family, especially my parents, who have provided all the support through all the time.

VITA OF XIAOFEN CHEN
March 2015

EDUCATION

Bachelor of Science, Wenzhou University, China, June 2003

Master of Medicine, Shanghai Jiao Tong University, China, March 2008

Master of Science, University of California, Santa Barbara, March 2015

PROFESSIONAL EMPLOYMENT

09/2003-03/2004 High School Teacher, Longgang High School, Wenzhou, China

04/2005-09/2005 Research Intern, Research Lab of Shanghai Golden Pharmaceutical Co. Ltd, Shanghai, China

09/2005-03/2008 Research Assistant, School of Pharmacy, Shanghai Jiao Tong University

02/2011-09/2012 Research Specialist, Department of Chemistry & Biochemistry, University of California, Santa Barbara

09/2012-09/2013 Research Assistant, Department of Chemistry & Biochemistry, University of California, Santa Barbara

09/2013-03/2015 Teaching Assistant, Department of Chemistry& Biochemistry, University of California, Santa Barbara

PUBLICATIONS

1. **X. Chen**, X. Liu, M. Burger, Y. Huang, G. C. Bazan, "Green-Solvent Processed Molecular Solar Cells," ***Angewandte Chemie***, 2014, DOI: 10.1002/ange.201409208.
2. H. Hou, **X. Chen**, J. Liu, X. Zhu, G. C. Bazan, B. E. Logan, "Repression of Hydrogen Uptake using Conjugated Oligoelectrolytes in Microbial Electrolysis Cells," ***International Journal of Hydrogen Energy***, 2014, DOI: 10.1016/j.ijhydene.2014.09.101
3. N. D, Kirchhofer, **X. Chen**, E. Marsili, J.J. Sumner, F. Dahlquist, G. C. Bazan, "The Conjugated Oligoelectrolyte DSSN+ Enables Exceptional Coulombic Efficiency via Direct Electron Transfer for Anode-Respiring Shewanella Oneidensis MR-1 -A Mechanistic Study," ***Phys. Chem. Chem. Phys***., 2014, 16, 20436-20443.
4. K. Sivakumar, V. B. Wang, **X. Chen**, G. C. Bazan, S. Kjelleberg, S. C. Loo, B. Cao, "Membrane permeabilization underlies the enhancement of extracellular bioactivity in Shewanella oneidensis by a membrane-spanning conjugated oligoelectrolyte, " ***Applied Microbiology and Biotechnology***, 2014.
5. V. B. Wang, N. D. Kirchhofer, **X. Chen**, M. Y. Tan, K. Sivakumar, B. Cao, Q. Zhang, S. Kjelleberg, G. C. Bazan, J. Loo, "Comparison of Flavins and a Conjugated Oligoelectrolyte in Stimulating Extracellular Electron Transport from Shewanella Oneidensis MR-1" **Electrochemistry Communications**, 2014, 41, 55-58.
6. J. Du, A. Thomas, **X. Chen**, C. Vandenberg, G. C. Bazan, "Increased Ion Conductance Across Mammalian Membranes Modified with Conjugated Oligoelectrolytes". ***Chem. Commun.***, 2013,49, 9624

7. H. Hou, **X. Chen**, A. W. Thomas, C. Catania, N. D. Kirchhofer, L. Garner, A. Han and G. C. Bazan, "Conjugated Oligoelectrolytes Increase Power Generation in E. coli Microbial Fuel Cells", ***Advanced Material***, 2013, 25, 1593-1597.

8. Z. B. Henson, P. Zalar, **X. Chen**, G. C. Welch. T-Q. Nguyen and G. C. Bazan. "Towards Environmentally Friendly Processing in Molecular Semiconductors''. ***J. Mater. Chem. A***, 2013, 1, 11117.

9. V. B. Wang, J. Du, **X. Chen**, et. al. "Improving Charge Collection in Escherichia Coli-carbon Electrode Devices Devices with Conjugated Oligoelectrolytes", ***Phys. Chem. Chem. Phys***., 2013, 15, 5867-5872.

10. **X. Chen**, Z. Liu, and Z. Mao, "Progress in Application of Chiral Phosphoric Acid in Asymmetric Synthesis", ***Progress in Chemistry*** (in Chinese), vol. 20 (10): 1534-1543, 2008.

ABSTRACT

Organic Semiconducting Molecules in Green Solvents

by

Xiaofen Chen

Conjugated oligoelectrolytes (COEs) contain a conjugated backbone and pendant groups with ionic functionalities. This unique structure combines the properties of semiconducting and water solubility. COEs have similar optical and electronic properties as compare to conjugated polyelectrolytes (CPEs), which have been widely studied for their unique combination of semiconductivity and water solubility, COE are relatively easier to be synthesized and purified. Certain COEs, such as DSBN+ and DSSN+, have been shown to spontaneously insert into liposomes and within the membranes of yeast, and to incorporate into the membranes of Escherichia coli leads to improvement of the current generation in MFCs. In order to study whether the structure variation would affect the biocompatibility of COEs and thus affect the performance of related devices, several new COEs in series with various conjugation length, molecular length, substitution groups with different electron withdrawing/donating group have been designed and synthesized.

Organic photovoltaics (OPV) have garnered a large amount of attention due to their potential for making light-weighted, flexible and low-cost devices in large scale application However, despite the power conversion efficiencies (PCEs) of OSC have steadily increased through improvements in materials design, mechanistic insight and device architectures, less

attention has been put on the sustainability of future application. The vast majority of high performing devices with bulk heterojunction (BHJ) structure are deposited out of chlorinated or aromatic solvents, such as chloroform and chlorobenzene, which require harsh preparation, costly clean up procedure. These solvents are quite toxic to environment and human being. Thus, to develop OSC system be processed out of alternative green solvents is of importance to the future application, especially in mass manufacturing. 2-MeTHF is used to process organic solar cell in the work. 2-MeTHF fits within the class of solvents sought from renewable resources and the concept of capitalizing on waste to generate useful chemicals. The power conversion efficiency of the solar cell processed out of 2-MeTHF is over 5%, which is quite decent and comparable to devices that processed out of chloroform. These findings open new opportunities for considering mass production of organic solar cells, and other optoelectronic devices. It also highlights that substantial molecular design may not be fundamentally necessary for opening environmentally benign processing.

TABLE OF CONTENTS

LIST OF FIGURES

Adv. Mater. **2013,** 25, 1593–1597-Partially reproduced by permission of The John Wiley and Sons http://onlinelibrary.wiley.com/doi/10.1002/adma.201204271/scheme 2.

Chapter 1. Design and Synthesis of New Conjugated Oligoelectrolytes (COEs)

1. Background and Motivation

π-Conjugated Oligoelectrolytes (COEs) contain a framework with electronic delocalized backbone and pendant groups with ionic functionalities. The π-conjugated backbone dictates electronic and optical properties, and semiconducting behavior; while the ionic pendant groups allow dissolution of COEs in aqueous media. This combination of semiconducting properties and aqueous solvent solubility allows for integration as biocompatibility of COEs with different applications. Such as in amplified biosensors, [1, 2] cell labeling and cell imaging, [3-5] as well as microbial fuel cells.[6]

Certain COEs, such as 4,4′-bis(4′-(*N*,*N*-bis(6′′-(*N*′,*N*′,*N*′-trimethylammonium) hexyl) amino)-styryl)stilbene tetraiodide (DSSN+, see scheme 1 for structure) has been studied and shown to interact with model bilayers and bacterial membranes, and thus to applied in various bio-based devices.[7-9] For example, it has been shown to integrate into yeast microbial fuel cells (MFCs) and facilitate the maximum current generated up to a five-fold increase. It has also been used to increase ion conductance across mammalian membrane. Also, it has also been illustrated to improve charge collection in Escherichia coli-carbon electrode devices.

Scheme 1-1. Structure of DSSN+

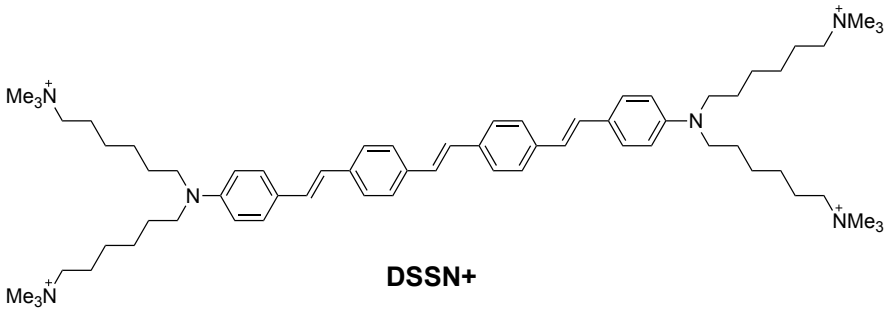

One of the proposed mechanism of how DSSN+ improves the performances of these devices is that the amphiphilicity of COEs leads to intercalate within lipid bilayer membranes in an ordered orientation, wherein the long axis of the conjugated backbone spans the membrane, so as to facilitate a more intimate electronic interaction between microorganisms and electrodes by enabling a transmembrane extracellular charge transfer. (Figure 1-1)

Figure 1-1. Spontaneous intercalation of DSSN+ into the membrane

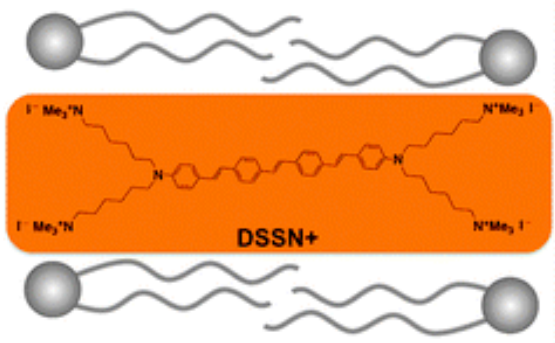

In order to exam whether various COEs structures will affect related devices performance, new COEs in series are designed and synthesized for systematic study. All of the molecules consist of a backbone of 3-5 phenylenevinylene repeat units with

terminal groups bearing ionic functionalities. The new COEs are designed to complete different series for variety: series 1 with different repeat unit in conjugate backbone, series 2 with different repeat unit in conjugated backbone as well, but use the O-pendant group instead of N-pendant group, to study whether different electron properties of O- will affect the molecule property, series 3 with electron withdrawing substituted, F, in the central aromatic ring in the backbone with N- pendant ionic and O- Pendant group separately, series 4 with carbonic as the ionic pendant group (see Scheme 2, 3, 4 and 5 for structures)

Scheme1-2. COEs series 1 with different repeat units in conjugated backbones

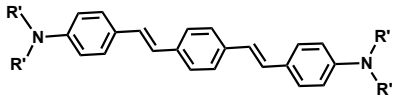

DSBN$^+$

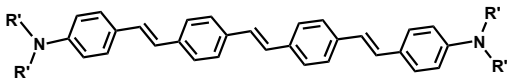

DSSN$^+$

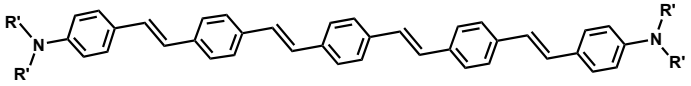

COE1-5C

R'= $(CH_2)_6N\overset{+}{M}e_3I^-$

Scheme 1-3. COEs series 2 with different repeat units in conjugated backbones

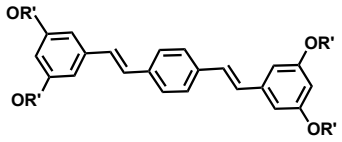

COE2-3C

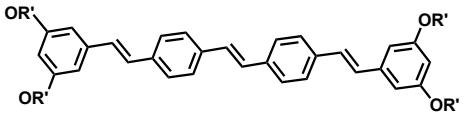

COE2-4C

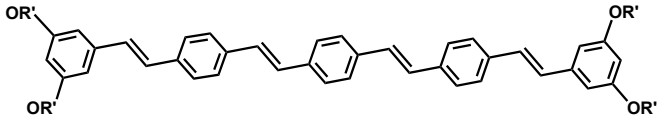

COE2-5C

R'= $(CH_2)_6N\,Me_3I^-$

Scheme 1-4. COEs series 3 with electron withdrawing substituted group in backbones

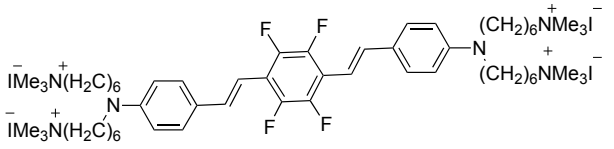

4F-COE1-3C

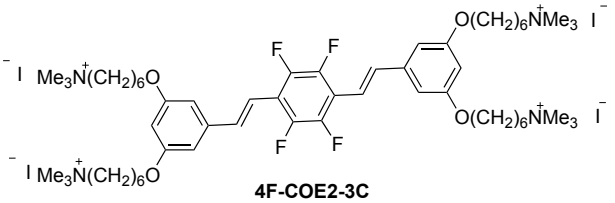

4F-COE2-3C

Scheme1- 5. COEs series 4 with carbonic ionic pending group

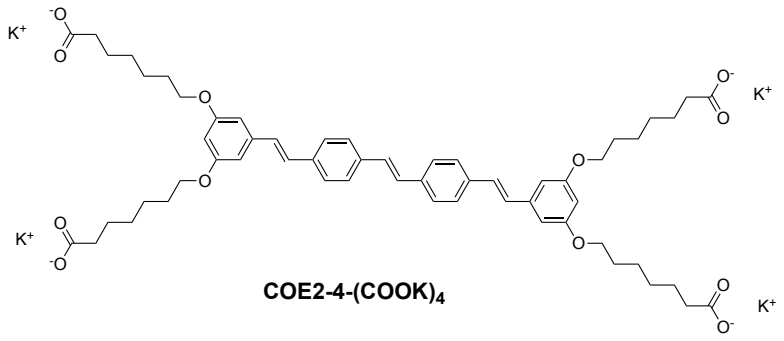

COE2-4-(COOK)$_4$

2. Optical Characterization of COEs

General optical properties of COEs were probed by using UV-vis absorption and photoluminescence (PL) spectroscopies. Figure1-2 shows the absorbance maxima of series 1 and 4F-COE1-3C. Figure 1-3 shows the absorbance maxima of series 2 and 4F-COE2-3C. Generally, with the extend backbone unit, the maxima absorbance tend to red-shifted.

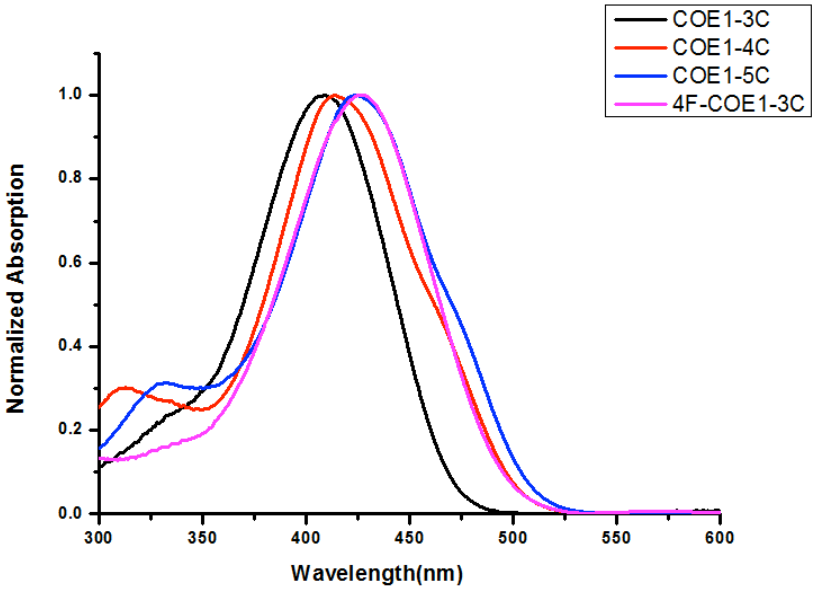

Figure 1-2 UV-vis absorption of series 1 and 4F-COE1-3C

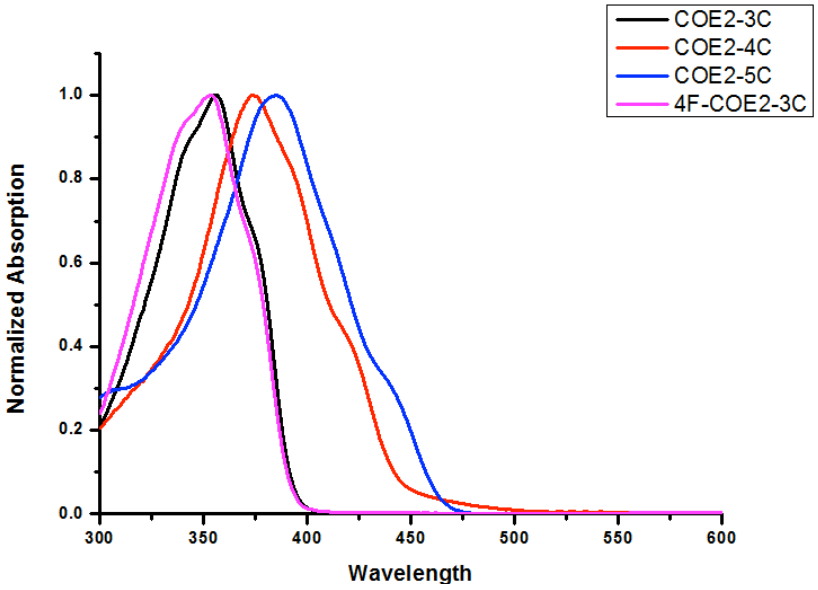

Figure 1-3 UV-vis absorption of series 1 and 4F-COE2-3C

3. Synthesis and Characterization of COEs

General Details. Chemicals were purchased from Aldrich Co. and were used without further purification. 1H and 13C NMR spectra were collected on a Bruker 500 MHz spectrometer. Mass spectrometry and elemental analysis were performed by UC Santa Barbara Mass Spectrometry Laboratory and Elemental Analysis Center. 1,4-Bis(diethylphosphonatemethyl)benzene and (E)-diethyl 4-(4-(bis(6-iodohexyl) amino)styryl)benzylphosphonate[6] were synthesized according to literature precedent.

General Sythesis method and Characterization. All COEs precursors are prepared via Horner-Wadsworth-Emmons reactions. The final ionic products are achieved by consecutive quaternization reactions of the precursors with trimethylamine in THF and then a second addition of trimethylamine in Methanol, DMSO or water. Both the neutral precursors and target chromophores were characterized by NMR spectroscopy, mass spectrometry and elemental analysis.

Scheme1-6. Synthetic Procedure for 4F-COE2-3N and 4F-COE2-3C

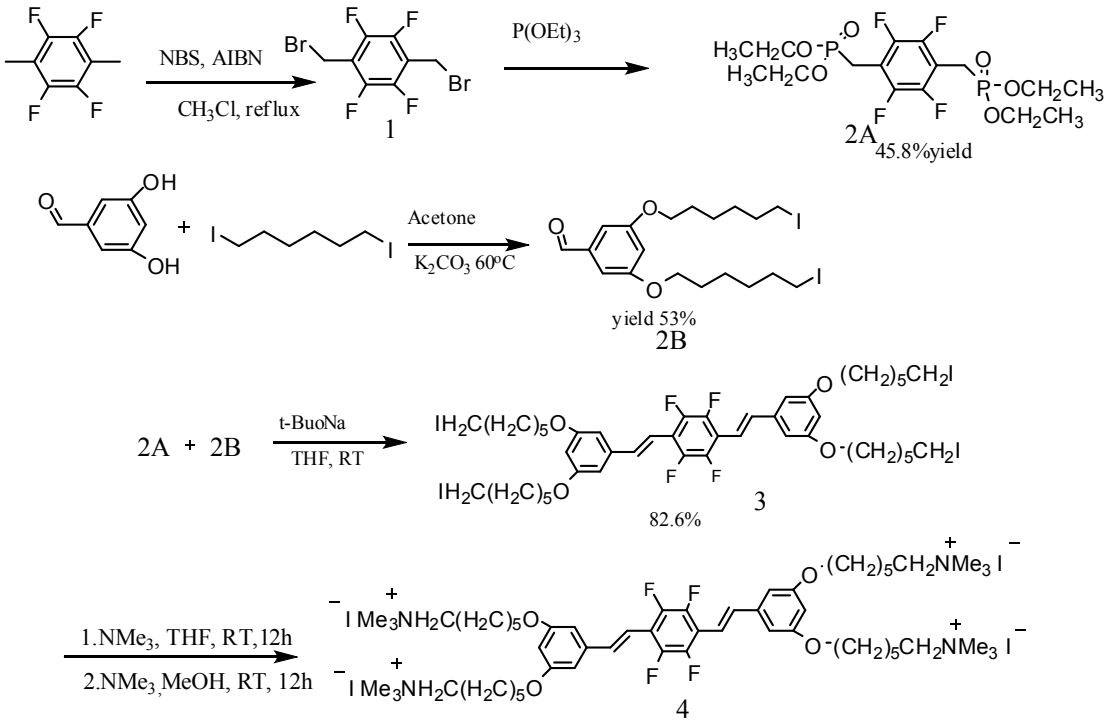

1,4-bis(bromomethy)tetrafluorobenzene(1). NBS(2.11g, 11.8mmol) and AIBN(2'2'-azobis (isobutyronitrile),0.034g,0.185mmol) were added to a stirred solution of 2,3,5,6-tetrafluoro-p-xylene(0.66g, 3.7mmol)in chloroform at room temperature. The mixture was heated to reflux for 16 hours. Then washed with water several time and brine once. The organic phase was dried through $MgSO_4$ and the solvent was distilled off via rota-vap. The crude product was purified by crystallized in ethanol to afford 0.523g of 1(yield 42.0%) as white solid.

1,4-Bis(tetrafluorobenzalphosphonate) (2A). Trimethyl phosphate(7ml) and 1,4-bis(bromomethyl)tetrafluorobenzene(1)(0.204g, 0.6mmol) were added to a flask and was heated to 95 ^{o}C for overnight. Distill trimethyl phosphate under vacuum, hexane

was then added to resulted mixture, solidify at freezer, white needles of 2A(0.125g, 45.8%yeild) were obtained through recrystallization of solid from ethanol.

1,4-Bis (3'5'-bis(6''-iodohexyloxy) styryl)-2,3,5,6-tetrafluorobenzene(3) A solution containing 153.4mg(0.341mmol) of the phosphonate(2A) and 437.5mg(0.784mmol,2.3eq) of the aldehyde 2B was added in dry THF. Then 68.7mg sodium tert-butoxide was added to the mixture, stirred overnight at room temperature. The solvent was evaporated while the remains was dissolved in dichloromethane and washed with water twice and brine once. The organic phase was dried through $MgSO_4$ and the solvent was distilled off via rota-vap. The crude material was purified by silica gel chromatography (dichloromethane/hexane=3:2) to afford 3 (354.2mg, 82.6% yield) in white solid.^{1}H NMR (500MHz, $CDCl_3$): 7.43, 7.40(d, J=16.5 Hz,2H), 7.06, 7.03(d, J=16.5 Hz,2H), 6.67(S,4H), 6.44(S,2H), 3.99(t, J=6.5Hz, 8H), 3.21(t, J=7.0Hz, 8H), 1.90-1.85(m, 8H), 1.84-1.80(m, 8H), 1.54-1.50(m, 8H). 13C NMR (500MHz, $CDCl_3$): 106.55, 138.71, 137.12, 114.45, 105.62, 102.10, 67.96, 33.44,30.95, 29.11, 25,14, 6.95). Anal. Calcd for: C46H58F4I4O4: C, 43.9; H, 4.65; N,0. Found: C, 44.1; H, 4.56; N: 0.096.

1,4-Bis(3'5'-bis(6''-N,N,N-trimethylammonium)hexyloxy)styryl)-2,3,5,6-tetrafluorobenzene tetraiodide (4) The neutral chromophores(3)(179.3mg) was dissolved in THF and the solution was cooled to -78C with dry ice/acetone bath. A large excess of condensed trimethylamine (~2ml)was added to the solution. The solution was allowed to warm to room temperature for 12 h and solvent was evaporated under vacuum. The residue was added methanol and another portion of condensed trimethylamine was added at -78^{o}C, the mixture was stirred for another 12 h for the

complete quaternization. Excess of ether was added to precipitate 4 (177.5mg,83.4% yield) in yellow-white powder. ^{1}H NMR(600MHz, in MeOH-d4): 7.43(d, J=17.4 Hz,2H), 7.10(d, J=17.4Hz, 2H), 6.71(S, 4H), 6.46(S,2H), 4.01(t, J=6, 8H), 3.35(t, J=7Hz, 8H), 3.12(S, 36H), 1.85-1.82(m, 16H), 1.62-1.59(m,8H), 1.48-1.45(m, 8H). ^{13}C NMR(500MHz, MeOH-d4):162.14, 140.03, 138.87, 115.12, 106.9, 103.6, 69.00, 67.91, 30.21, 27.17, 26.84, 24.00. Anal. Calcd for C59H94F4N4O4: C, 46.6; H, 6.34; N, 3.75. Found: C,46.0; H, 6.30; N, 3.66.

Scheme 1-7. Synthetic Procedure for 4F-COE1-3N and 4F-COE1-3C

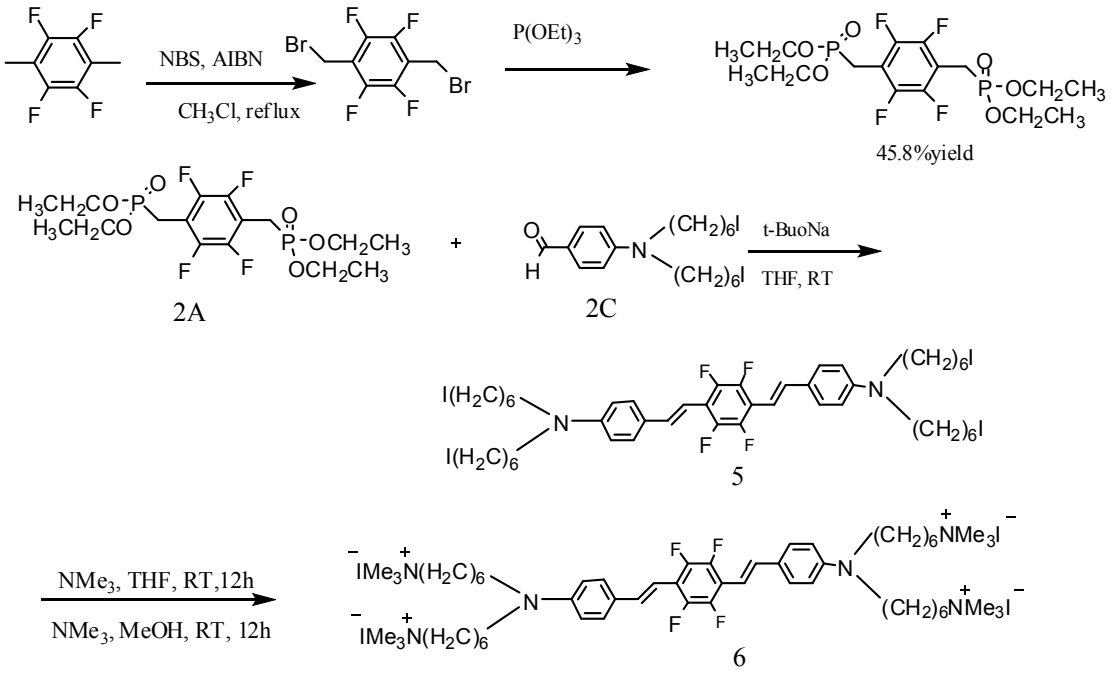

1,4-Bis(4'-(N,N-bis(6''-iodohexyl)amino)styryl)-2,3,5,6-tetrafluorobenzene (4F-COE1-3N, 5):

A solution containing 153.4mg(0.341mmol) of the phosphonate (2A) and 2.3eq of the aldehyde 2C was added in dry THF. Then 68.7mg sodium tert-butoxide was added to the mixture, stirred overnight at room temperature. The solvent was evaporated while the remains was dissolved in dichloromethane and washed with water twice and brine once. The organic phase was dried through $MgSO_4$ and the solvent was distilled off via rota-vap. The crude material was purified by silica gel chromatography (dichloromethane/hexane=3:2) to afford 5 in white solid.^{1}H NMR (500MHz, $CDCl_3$): 7.417, 7.402(d, J=7.5Hz, 4H), 7.408, 7.402(d, J=13.5Hz, 2H), 6.859,6.832(d, J=13.5Hz, 2H), 6.628, 6.613(d, J=7.5Hz, 4H), 3.319-3.293(t, J=6.5Hz, 8H), 3.213-3.190(t, J=6.0Hz, 8H), 1.870-1.822(m, 8H), 1.641-1.591(m, 8H), 1.486(m, 8H), 1.390-1.339(m, 8H)

1,4-Bis(4'-(N,N-bis(6''-(N,N,N-trimethylammonium)hexyl)amino)styryl)-2,3,5,6-tetrafluorobenzene tetraiodide (4F-COE1-3C, 6): The neutral compound 4F-COE1-3N was dissolved in THF and then cooled to -78^{o}C with dry ice/acetone bath. A large excess of condensed trimethylamine (~2ml)was added to the solution. The solution was allowed to warm to room temperature for 12 h and THF was evaporated under vacuum. The residue was then added small amount of H_2O to dissolve the first precipitate and then treat the system with trimethylamine, after stirring for 12h, add excess of THF to precipitate.

^{1}H NMR(600MHz, MeOH-d4): 7.39(d, J=9Hz, 4H), 7.35(d, J= 16.8Hz, 2H), 6.85(d, J=16.8Hz, 2H), 6.72(d, J=9Hz, 4H), 3.41-3.14(m, 16H), 3,14(S, 36H), 1.84-1.80(m, 8H), 1.69-1.65(m, 8H), 1.50-1.47(m, 16H)

Scheme 1-8. Synthetic Procedure for **COE2-4-(CN)$_4$** and **COE2-4-COOK**

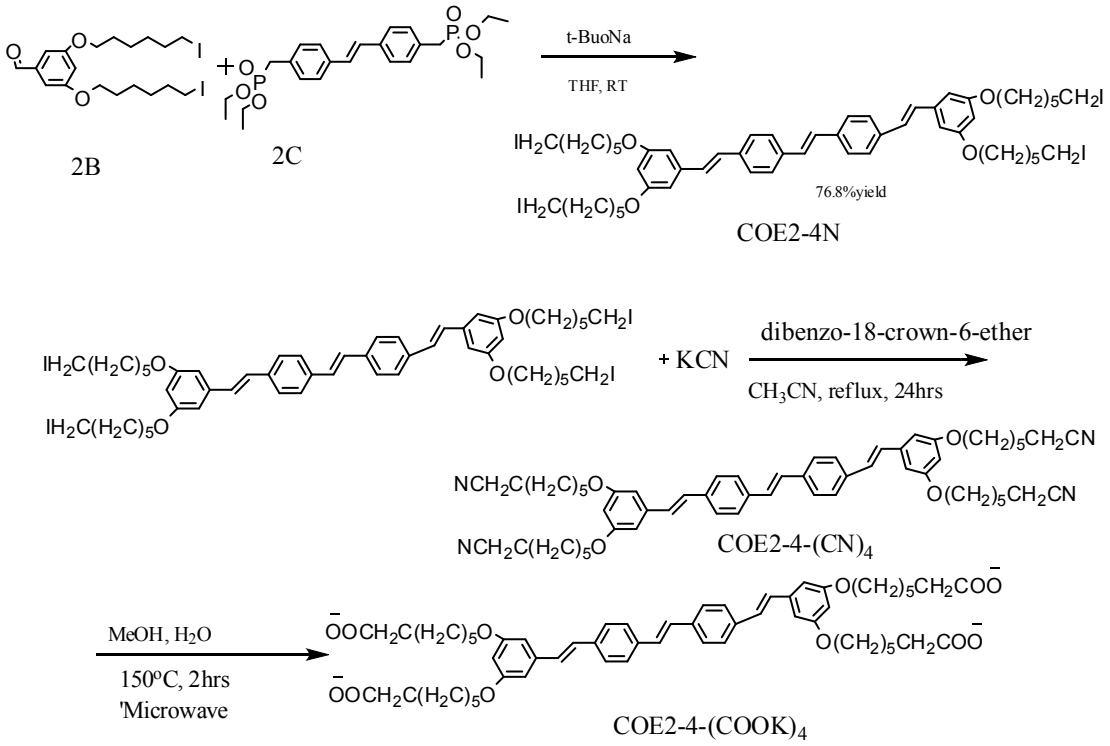

COE2-4N: A solution containing 156mg(0.325mmol) of the phosphonate (2C) and 400mg(0.717mmol,2.3eq) of the aldehyde 2B was added in dry THF. Then 47.1mg sodium tert-butoxide was added to the mixture, stirred overnight at room temperature. The solvent was evaporated while the remains was dissolved in dichloromethane and washed with water twice and brine. The organic phase was dried through $MgSO_4$ and the solvent was distilled off via rota-vap. The crude material was purified by silica gel chromatography (dichloromethane/hexane=3:2) to afford COE2-4N (321.5mg, 76.8% yield) in yellow powder.

COE2-4-(CN)$_4$: In a 250ml round flask, add 202mg(0.16mmol)COE2-4N, 210mg(3mmol,20eq)KCN, and 60mg dibenzo-18-crown-6-ether, then add 150ml acetonitrile. Heat up the mixture to 90^{o}C and run for 24 hours. The solvent was distilled off while the remains was dissolved in dichloromethane and washed with water and

brine. The organic phase was dried through $MgSO_4$ and the solvent was distilled off via rota-vap. The crude was purified by silica gel chromatography to afford COE2-4-$(CN)_4$ in yellow powder.

^{1}H NMR (500MHz, $CDCl_3$): 7.5(d, 8H), 7.125(S, 2H), 7.1-7.0(d,d,$J_{1,3}$=23.5, $J_{1,2}$=16.5, 4H), 6.66(S, 4H), 6.37(S,2H), 4.01(t, J=7.2Hz, 8H), 2.38-2.35(t, J=7, 8H), 1.85-1.82(m, 8H), 1.74-1.71(m, 8H), 1.58-1.53(m, 16H). 13CNMR: 160.40, 139.33, 136.81, 136.58, 128.73, 128.62, 128.22, 126.94, 126.87, 119.72, 105.19, 67.71, 29.01, 28.44, 25.42, 25.34, 17.12

COE2-4-COOK: ^{1}H NMR (500MHz,MeOD-d4): 7.552(s, 8H), 7.194(S, 2H), 7.12(d,d,J2,3=5.4, 4H), 6.69(d, J=2Hz, 4H), 6.37(S,2H), 3.98(t, J=6.5Hz, 8H), 2.18(t, J=6.5Hz, 8H), 1.86-1.76(m, 8H), 1.68-1.62(m, 8H), 1.45-1.39(m, 8H)

Scheme 1-9. Synthetic Procedure for **COE2-5N** and **COE2-5C**

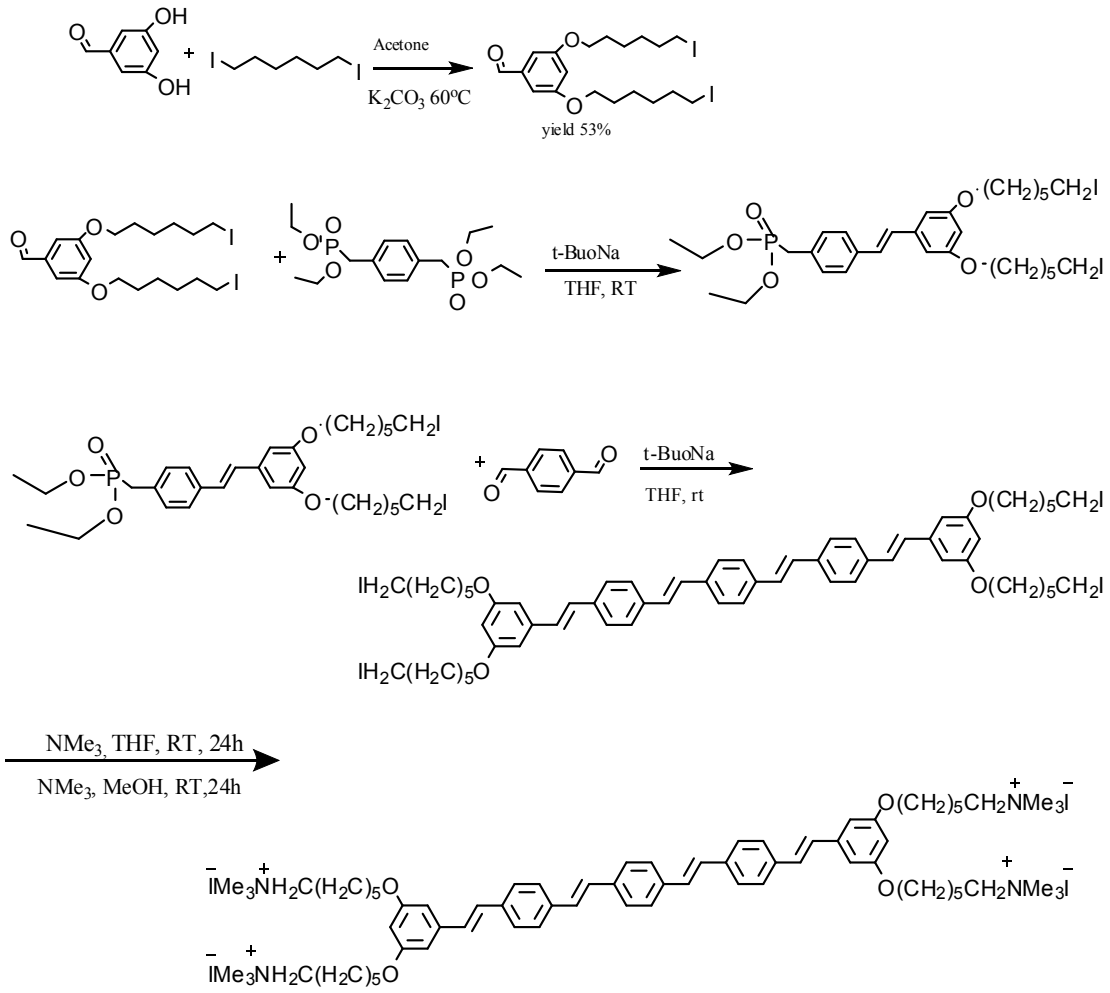

(E)-diethyl 4-(3,5-bis(6-iodohexyloxy)styryl)benzylphosphonate: A solution containing 650mg(1.16mmol) of the aldehyde **1** and 528.6mg(1.39mmol, 1.2eq) of the phosphonate**2** was added in dry THF. Then 122.6mg sodium tert-butoxide was added to the mixture, stirred overnight at room temperature. The solvent was evaporated while the remains was dissolved in dichloromethane and washed with water twice and brine. The organic phase was dried through $MgSO_4$ and the solvent was distilled off via rota-

vap. The crude material was purified by silica gel chromatography (chloromethane/ethyl acetate =9:1) to afford 223mg **4** in yellow powder (24.5%yield). ^{1}H NMR (500 MHz, $CDCl_3$): δ 7.46 (d, *J* = 8 Hz, 2H), 7.29 (d, *J* = 8 Hz, 2H, doublet is split presumably due to coupling to phosphorous), 7.04 (d, *J* = 16 Hz, 1H), 6.98 (d, *J* = 16 Hz, 1H), 6.63 (m, 2H), 6.37 (m, 1H), 4.01 (m, 4H), 3.97 (t, 4H), 3.20 (t, 4H), 3.14 (d, 2H), 1.86 (m, 4H), 1.79, (m, 4H), 1.49 (m, 8H), 1.26 (t, 6H).

1,4-bis(4-(3,5-bis(6-iodohexyloxy)styryl)styryl)benzene(COE2-5N): A solution containing 12.2 mg (0.09mmol) of the terephthalaldehyde and 156mg (0.2mmol, 2.2eq) of the phosphonate(**4**) was added in dry THF. Then 19.2mg sodium tert-butoxide was added to the mixture, stirred overnight at room temperature. The solvent was evaporated while the remains was dissolved in dichloromethane and washed with water twice and brine. The organic phase was dried through $MgSO_4$ and the solvent was distilled off via rota-vap. The crude material was purified by silica gel chromatography (dichloromethane/hexane) to afford **COE2-5N** 77mg (60.9% yield) in yellow powder. m/z= 1390.0 ^{1}H NMR (500 MHz, CD_2Cl_2): δ 7.51 (m, 12H, singlet atop a set of coupled doublets), 7.13 (s, 4H), 7.08 (d, *J* = 16.5 Hz, 2H), 7.04 (d, *J* = 16.5 Hz, 2H), 6.66 (d, *J* = 2 Hz, 4H, splitting presumably due to meta coupling), 6.38 (t, *J* = 2 Hz, 2H, splitting presumably due to meta coupling), 3.99 (t, 8H), 3.22 (t, 8H), 1.86 (m, 8H), 1.80 (m, 8H), 1.53 (m, 16H). ^{13}C (800 MHz, CD_2Cl_2): δ 159.97, 138.64, 136.25, 136.20, 136.05, 128.02, 127.90, 127.53, 127.50, 126.33, 126.3, 126.29, 104.43, 100.41, 67.36, 32.98, 29.71, 28.54, 24.51, 6.66. FD-MS: 1390 (M^+), 695 (M^{2+}). Elemental analysis (CHN) calculated: C, 53.54; H, 5.36; N, 0. Found: C, 54.0; H, 5.31; N, 0.23.

1,4-bis(4-(3,5-bis(6-(trimethylammonium)hexyloxy)styryl)styryl)benzene tetraiodide(COE2-5C) The neutral compound **COE2-5N** was dissolved in THF and then cooled to -78^{o}C with dry ice/acetone bath. A large excess of condensed trimethylamine(~2ml)was added to the solution. The solution was allowed to warm to room temperature for 12 h and THF was evaporated under vacuum. The residue was then added small amount of H_2O to dissolve the first precipitate and then treat the system with trimethylamine, after stirring for 12h, add excess of THF to precipitate. **COE2-5C** was obtained as yellow solid (yield= 83.5%). ^{1}H NMR (500 MHz, DMSO-d_6): δ 7.62 (m, 12H, singlet atop a set of coupled doublets), 7.31 (s, 4H, overlaps with doublet at 7.29 ppm), 7.29 (d, 2H, overlaps with singlet at 7.31 ppm), 7.21 (d, J = 16 Hz, 2H), 6.78 (m, 4H), 6.40 (m, 2H), 4.01 (t, 8H), 3.31 (m, 8H), 3.05 (s, 36H), 1.72 (m, 16H), 1.49 (m, 8H), 1.37 (m, 8H). ^{13}C NMR (800 Mhz, DMSO-d_6): δ 159.93, 139.00, 136.44, 136.38, 136.19, 128.39, 128.30, 127.91, 127.89, 126.83, 126.53, 126.20, 104.78, 100.59, 67.28, 65.24, 52.17, 28.38, 25.40, 25.02, 21.95. ESI/TOF-MS: 686 ((M-2I)$^{2+}$), 415 ((M-3I)$^{3+}$), 279 ((M-4I)$^{4+}$). Elemental analysis (CHN) calculated: C, 54.62; H, 6.81; N, 3.44. Found: C, 54.0; H, 6.99; N, 3.30.

4. References

1. Z. Chen, X.-D. Dang, A. Gutacker, A. Garcia, H. Li, Y. Xu, L. Ying, T.-Q, Nguyen, G. C. Bazan, J. Am. Chem. Soc. **2010**, *132*, 12160-12162.
2. D. Wand, X. Gong, P. S. Heeger, F. Rininsland, G. C. Bazan, A. J. Heeger, Proc, Natl. Acad. Sci. **2002**, *99*, 49.
3. A. Herland, K. P. R. Nilsson, J. D. M. Olsson, P. Hammarstrom, P. Konardsson, O. Inganas, J. Am. Chem. Soc. **2005**, *127*, 2317.
4. K. –Y. Pu, K. Li, X. Zhang, B. Liu, Adv. Mater. **2010**, *22*,4186.
5. A. Duarte, A. Chworos, S. F. Flagan, G. Hanarhan, G. C. Bazan, J. Am. Chem. Soc. **2010**, *132*, 12562.
6. L. E. Garner, J. Park, S. M. Dyar, A. Chworos, J. J. Summer and G. C. Bazan, J. Am. Chem. Soc., **2010**, *132*,10042.
7. L. E. Garner, A. W. Thomas, J. J. Sumner, S. P. Harvey and G. C. Bazan, Energy Environ. Sci. **2012**, *5*, 9449.
8. V. B. Wang, J. Du, X. Chen, A. W. Thomas, N. D. Kirchhofer, and L. E. Garner, et al. Phys, Chem. Chem. Phys. **2013**, *15*, 5867.
9. A. W. Thomas, L. E. Garner, K. P. Nevin, T. L. Woodard, A. E Franks and D. R. Lovely, et al. Energy Environ. Sci. **2013**, *6*, 1761.

Angew. Chem., **2014**,126: 14606–14609.-Reproduced by permission of The John Wiley and Sons. http://onlinelibrary.wiley.com/doi/10.1002/ange.201409208/full

Chapter 2. Green-Solvent Processed Molecular Solar Cells

1. Background of processing solvents in OSCs fabrication

Renewable energy and environmental protection are of importance to the sustainable development of technology, especially for mass manufacturing, using non-toxic and chemically sustainable resources is a very important merit.[1–3] Organic solar cells (OSCs) produced via solution processing are a relevant case in point. Organic solar cells have garnered a large amount of attention due to their potential for making light-weighted, flexible and low-cost devices in large scale. Through decades of effort input, excellent power conversion efficiencies (PCE) have been achieved. Polymer solar cells have reached over 10% PCE and small molecule solar cells are approaching about 8%. But much less effort has been put into the sustainable development of future application.[4-8] Despite that the power conversion efficiencies (PCEs) of OSCs have steadily increased through improvements in materials design,[9–14] mechanistic insight,[15–19] and device architectures,[20–22] the vast majority of high performing devices with bulk heterojunction (BHJ) structures are deposited out of chlorinated and/or aromatic solvents, *e.g.*, chlorobenzene, 1,2-dichlorobenzene(o-DCB), and chloroform(CF). This class of solvents is produced from

non-renewable resource, which accelerates resource depletion. They usually demand harsh and harmful procedures for production, which increases the cost of production and risk of explosion. In addition, they usually introduce pollution and damage to environment.[23–26] It is worth noting that regulations are being enacted, particularly in the European Union, that have as a long term goal of the elimination of harmful and unsustainable chemicals and materials.[3] These emerging restrictions are worthwhile to consider even at the basic level of research, not only when they apply to the photoactive materials themselves, but equally importantly to any chemical intermediates and fabrication options. This is particularly true considering that one of the important motivations for solar cell is to be low-cost and potentially environmentally benign, compare to traditional energy resources. Despite the importance of the matter, there is few work focus on developing environmentally friendly processed organic photovoltaics.

The BHJ active layer comprises of a blend of a donor material (either conjugated polymer or small molecule, D) and an acceptor material (most typically a fullerene derivative, A).[27-30] In general, the construction of nanoscale bi-continuous phase-separated domains of tens of nanometers are one of the key procedures in high-performance bulk heterojunction (BHJ) based devices. A variety of physical phenomena restrict the dimensions of the film and the possible domain sizes of the donor and acceptor phases. Best performance is achieved when optimal percolation pathways are available for the holes and electrons to reach the corresponding charge collecting electrodes. Furthermore, ordered domains in the donor phase are important for maximizing hole mobilities and promoting phase separation.[31-32] Ideally, one would like to achieve these morphological requirements during the film deposition process and therefore solvent, temperature, substrate and possible solvent additives are critical considerations since these variables influence the kinetic profile of film

formation. Choosing the right solvent is the initial and the most critical step. Among the reported high performance BHJ solar cells, halogenated aromatic solvents like CB and o-DCB and halogenated alkane solvent like CF are the most frequently used ones due to their superior solubility for nonpolar organic molecules and fullerene derivatives, as well as other desirable physical properties such as relatively high boiling points, and high viscosity. Research efforts have been recently put into other solvent substitutes such as non-aromatic and non-halogenated which are compatible with environmental impact concerns and thus are preferred in mass application[4-7]. However, those successes are still very limited.

2. Motivation of using green solvents for OSCs processing

To consider the sustainable developments point of view which requires using more renewable resources of the planet and reducing environment impact, Also in the light of the "green chemistry" application which requires the design of chemical product and process that reduce or eliminate the use and generation of hazardous substance, the ability to process organic semiconductors from green solvents will be of great importance in the progress of industrializing OPV at a lower environmental and financial cost.

Solvents such as *N*-methyl-2-pyrrolidone[33] and alcohol[34] have appeared in the literature. By using conjugated polymers with side groups that increase solubility in more polar solvents, one can develop OSCs systems that can be processed in more environment friendly solvents. However, the extent to which these side groups influence solid state morphology, for example miscibility with fullerene derivatives, is not well understood. It seems reasonable to us that molecules with less extended structures would be attractive candidates

for exploring casting active BHJ from green solvents given their greater solubility, relative to macromolecular counterparts.

3. Choose 2-MeTHF as OSCs processing solvent

In order to developed green solvent processed organic solar cell system, we have to first screen the green solvent candidate. The solvent is selected among Methanol, Ethanol, Ethyl Acetate, Ether and 2-MeTHF. For the alternative solvent, it must have reasonable solubility for both donor and acceptor materials in order to make decent thin film. For each solvent, we test the potential donor and acceptor materials' solubility by UV-vis spectroscopy. It turns out, within all the candidates, 2-MeTHF has the largest solubility for most of the donor and acceptor materials we have synthesized in Bazan group.

2-MeTHF can be obtained from furfural, which is derived from agricultural by-products, such as corncobs, oat, wheat bran, and sawdust.[35, 36] see scheme 2-1 for the 2-MeTHF industrialized production method. It fits within the class of solvents sought from renewable resources and the concept of capitalizing on waste to generate useful chemicals.

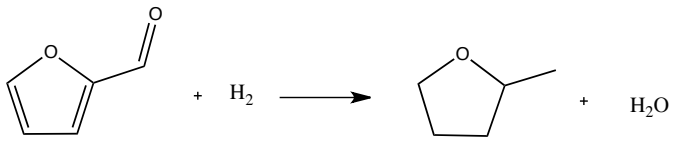

fufural **2-MeTHF**

Moreover, the toxicity of 2-MeTHF is lower than that of commonly used halogenated and aromatic solvents such as chlorobenzene and chloroform.[37] These motivations have led to reports that highlight the interest in 2-MeTHF as a green solvent substitute in organic

syntheses applications including organocatalysis, biotransformations and pharmaceutical chemistry.[38–40]

4. Devices fabrication and characterization

It seemed reasonable to examine X2 as the molecular donor; see Scheme 2-2 for molecular structure. This material exhibits high thermal stability and crystallinity together with good solubility in non-polar solvents.[41]Two additional points for the fabrication of solar cells are relevant. First, PCEs on the order of 6.5 % have been achieved with blends of X2 with [6, 6]-phenyl-C_{61}-butyric acid methyl ester ($PC_{61}BM$) from $CHCl_3$ in the absence of solvent additives. Second, the PCE values are maintained at similar levels across a range of D:A (wt:wt) compositions from 7:3 to 4:6; the BHJ performance is thus relatively resistant to compositional variations.[42] An initial set of tests demonstrated that the room temperature solubility of X2 in 2-MeTHF is approximately 29 mg/mL, which proved sufficient for casting films of more than 300 nm thickness.

Scheme 2-2. Molecular Structures of X2, bis$PC_{61}BM$, $PC_{61}BC_8$, and 2-MeTHF

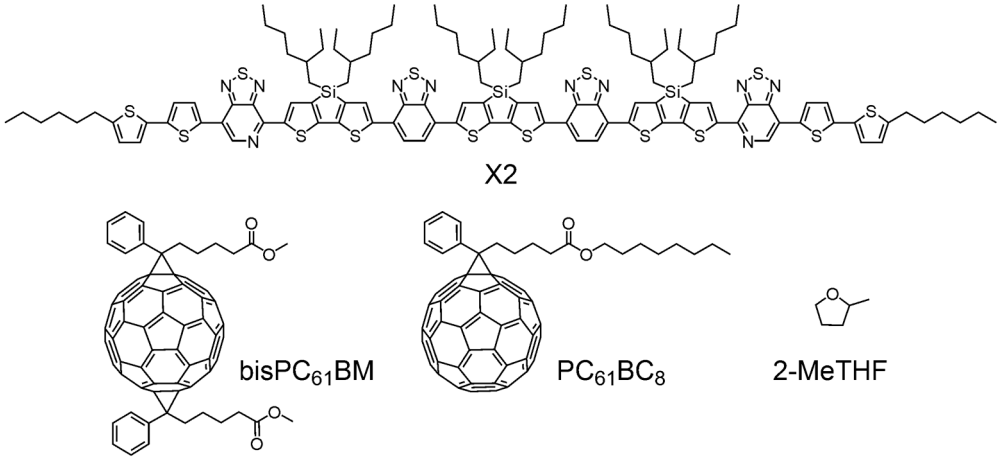

With respect to the fullerene acceptor, the solubility of widely used $PC_{61}BM$ in 2-MeTHF was determined to be less than 1 mg/mL, too low for effective thin film deposition via spin coating. We thus examined the doubly substituted bis$PC_{61}BM$ and a $PC_{61}BM$ derivative with a longer alkyl chain, $PC_{61}BC_8$ and found that their solubility were higher than 15 mg/mL and 9 mg/mL, respectively. Our initial efforts to screen device performances with the X2:bis$PC_{61}BM$ combination demonstrated consistently poorer performance relative to the X2:$PC_{61}BC_8$ blends. The best PCE obtained for X2: bis$PC_{61}BC_8$ blends out of 2-MeTHF is 2%. (*J-V* curve see Figure 2-1). Compare the device parameters of X2: bis$PC_{61}BC_8$ to previous devices of X2: PCBM shows that the Jsc are relatively low. In order to increase Jsc, PS is applied to increase the viscosity of the solution and thus to increase the thickness of active layer. As expected, data shows PS can increase the average of the active layer thickness from 99 nm to 118 nm (with 1% PS) and 122 nm (2% PS), Jsc thus increased a little bit, but not significant enough to improve the devices performance. Emphasis was therefore placed on examination of the X2:$PC_{61}BC_8$ blend.

Table 2-1: Comparison of device performance of X2: bisPCBM processed in chloroform and 2-MeTHF and with different concentration of PS additive

Solvent /additive	J_{sc} [mA /cm^2]	V_{oc} [V]	FF [%]	PCE [%]
CF	7.51	0.80	40	2.4
2-MeTHF	4.9	0.77	35	1.3
2-MeTHF w/1% PS	5.21	0.78	40	1.83
2-MeTHF w/2%PS	5.24	0.78	38	1.55

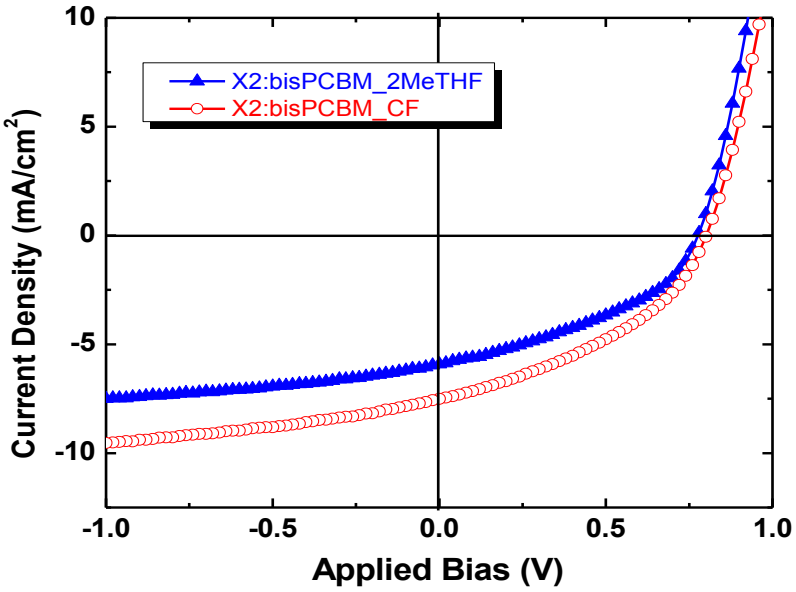

Figure 2-1: (a) *J-V* characteristics of the optimal performance measured from films of **X2**:bisPCBM prepared from 2-MeTHF (triangles) and $CHCl_3$ (circles) under illumination (simulated AM 1.5G), with total concentration of 30 mg/mL, 50:50, wt/wt. For film blend out of 2-MeTHF, show the best PCE of 2%, with *Jsc*=5.65 mA/cm^2, *Voc*=0.78 V, and FF = 46%; for film blend out of chloroform (CF), show the best PCE of 2.7%, with *Jsc*=7.14 mA/cm^2, *Voc* = 0.8 V, and FF = 48%.

Our investigation starts from the UV-vis absorption spectra of the blend films. As shown in Figure 2-2, blend films with X2/$PC_{61}BC_8$ cast from 2-MeTHF and $CHCl_3$ show almost identical absorption characteristics between the 300-900 nm range, which are also very similar to that observed with X2/$PC_{61}BM$ films prepared from $CHCl_3$.[42]

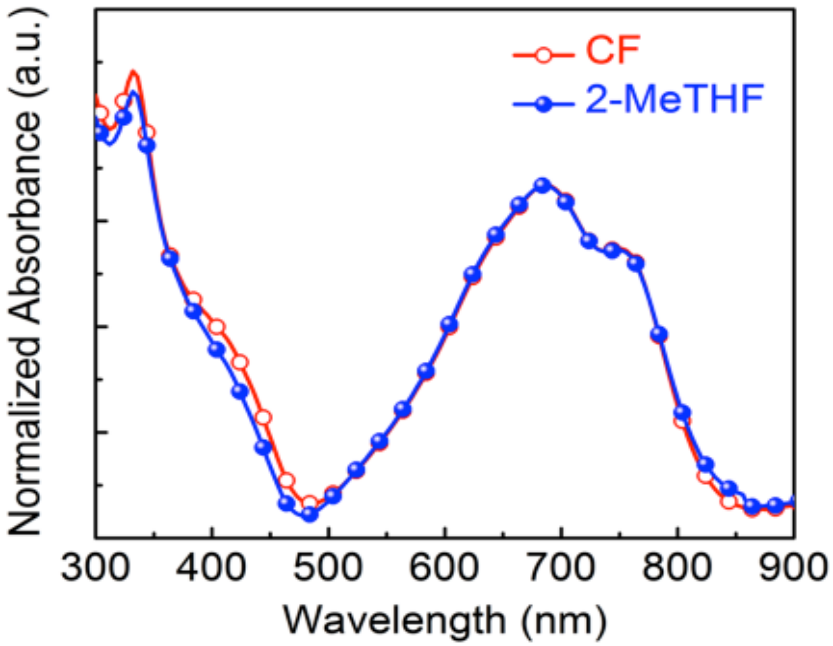

Figure 2-2. Thin film UV-vis absorption spectra of 50:50 X2:$PC_{61}BC_8$ blend obtained from 2-MeTHF (blue spheres) and $CHCl_3$ (red circles) from solutions containing 25 mg/mL total semiconductor content.

The surface roughness and film morphology, as determined by atomic force microscopy (AFM), are also not greatly affected by the choice of solvent (see Figure 2-3). These characterizations tools thus do not reveal any obvious differences in possible changes in surface features or film quality that would be detrimental factors for device fabrication.

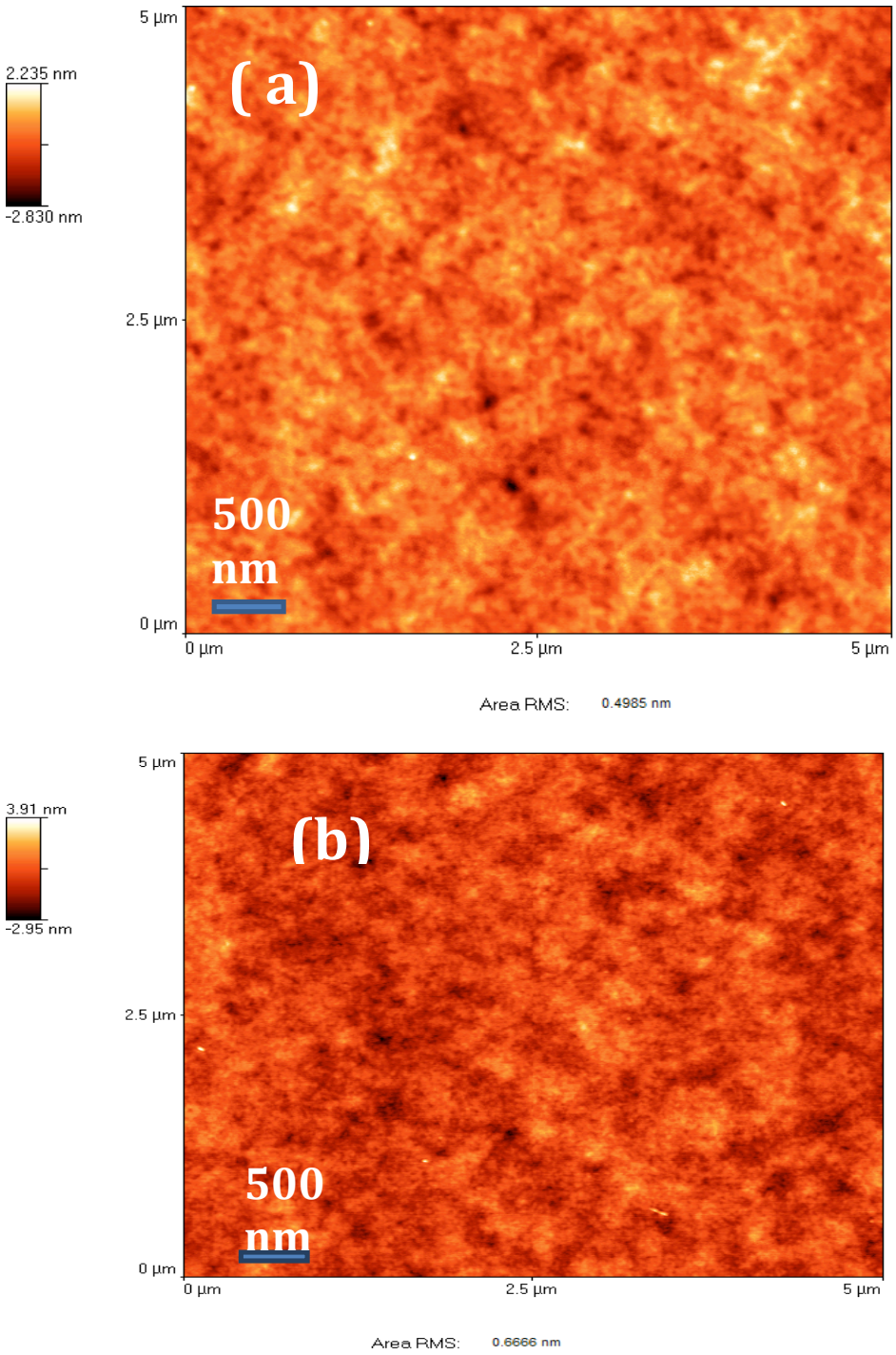

Figure 2-3: Topographic height images (5×5 μm^2) determined by atomic force microscopy of **X2**:$PC_{61}BC_8$ films obtained from (a) 2-MeTHF, (b) $CHCl_3$.

Hole-only diodes were fabricated to understand whether the charge-transporting properties of the BHJ films would be changed when processed from 2-MeTHF.

Molybdenum oxide (MoO_x) was chosen as the bottom contact since it has a deeper work function than the highest occupied molecular orbital (HOMO) of X2. Gold was chosen as the top contact to minimize electron injection e since it has a work function deeper than the lowest unoccupied molecular orbital (LUMO) of $PC_{61}BC_8$.[43, 44] The current density-voltage characteristics (*J-V)* in the dark (see Figure 2-4) were collected and the Mott-Gurney law for the space-charge-limited-current (SCLC) was used to determine the zero field mobility of the layer according to the following equation:[45]

$$J = \frac{9}{8}\varepsilon\varepsilon_0\mu_0\frac{V^2}{L^3}$$

where ε is the material's dielectric constant, ε_0 is the permittivity of vacuum, V is the applied bias, L is the film thickness, J is the measured current density and μ_0 is the zero field mobility of the material being determined.

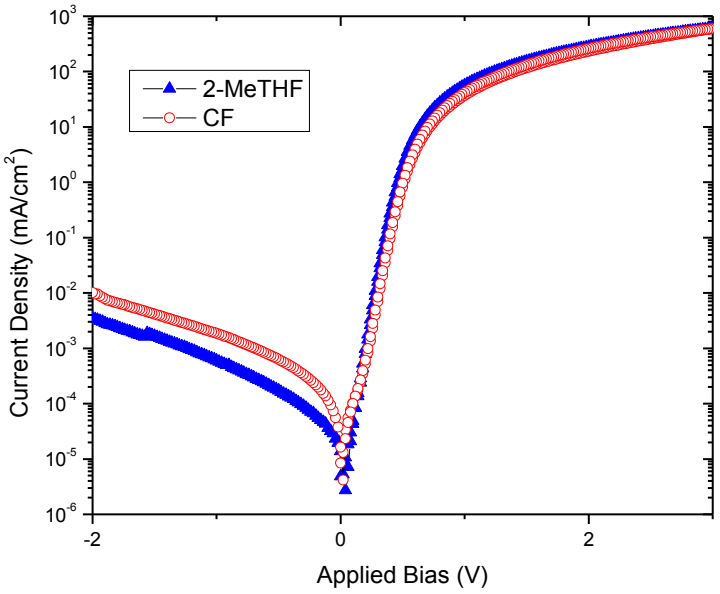

Figure 2-4: The Current density-voltage characteristics (*J-V*) in the dark for hole-only devices processed out of $CHCl_3$ (circles) and 2-MeTHF (triangles).

Analysis of the results provided in Figure 2-5 provided hole mobilites for the blends prepared from $CHCl_3$ and from 2-MeTHF of 2.1×10^{-4} cm^2 V^{-1} s^{-1} and 5.6×10^{-4} cm^2 $V^{-1}s^{-1}$, respectively. Indeed, the film cast from 2-MeTHF exhibited slightly higher hole mobility, a desirable quality for extraction of photoinduced charge carriers in photovoltaic devices. [46]

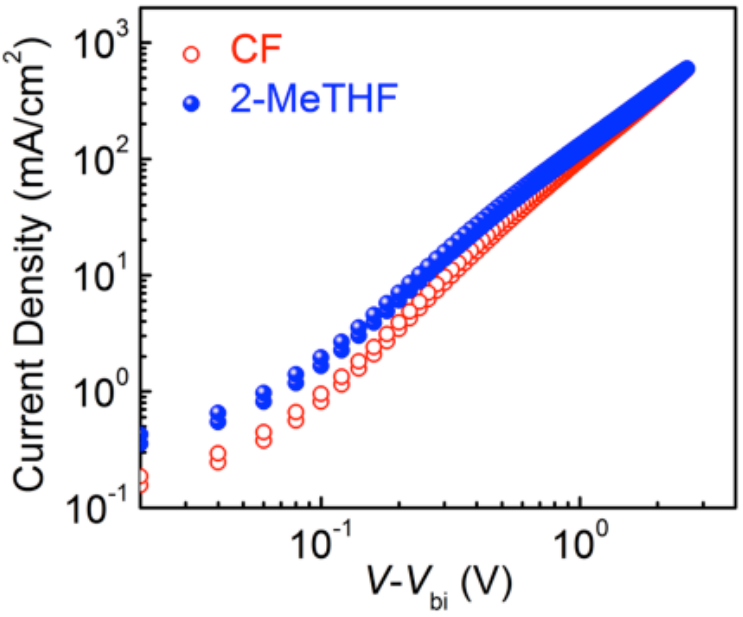

Figure 2-5. Current density of X2:$PC_{61}BC_8$ blend films (25 mg/mL total concentration, D:A= 50:50, wt/wt) prepared from $CHCl_3$ (circles) and 2-MeTHF (spheres).

BHJ devices fabricated with X2:$PC_{61}BC_8$ films processed from either $CHCl_3$ or 2-MeTHF and were characterized in parallel to investigate the photovoltaic properties. The device structure adopted for our studies is ITO/MoO_x/X2:$PC_{61}BC_8$/Ca/Al, where ITO is indium tin oxide and MoO_x is molybdenum oxide prepared by thermal evaporation.

Examination of previous work[42] led us to focus on the fabrication of X2:$PC_{61}BC_8$ with 60:40 and 50:50 ratios. As shown in Table 2-2, these two ratios provide devices with very similar characteristics.

processing solvent	D:A ratio	J_{sc} [mA /cm^2]	V_{oc} [V]	FF [%]	PCE [%]
$CHCl_3$	6:4	10.9	0.70	54	4.1
	5:5	10.4	0.72	61	4.6
2-MeTHF	6:4	11.1	0.70	55	4.3
	5:5	10.7	0.72	59	4.5

Table 2-2: Comparison of device performance with 20 mg/ mL total concentration with D:A ration between 60:40 and 50:50, wt/wt.

To get the consistence of devices data, more than 20 devices are made under same conditions. Table 2-3 provides a summary of device characteristics, the average values correspond to examination of at least 20 devices. Both in $CHCl_3$ and 2-MeTHF with different total concentration.

solvent/ concentration (mg/mL)		J_{SC} (mA /cm^2)	V_{OC} (V)	FF (%)	PCE (%)	
					Best	Avg.
$CHCl_3$	20	9.6 ± 0.3	0.72 ± 0.02	62 ± 1	4.5	4.3
	25	11.5 ± 0.3	0.72 ± 0.01	54 ± 2	4.7	4.6
	30	12.3 ± 0.2	0.71 ± 0.03	52 ± 2	4.7	4.6
2-MeTHF	20	10.3 ± 0.2	0.72 ± 0.02	59 ± 2	4.6	4.4
	25	12.3 ± 0.2	0.72 ± 0.02	55 ± 1	5.1	4.8
	30	12.5 ± 0.3	0.72 ± 0.02	53 ± 2	4.9	4.7

Table 2-3. Photovoltaic Properties of Devices Processed out of Different Solvents at Different Concentrations (X2:$PC_{61}BC_8$ = 50:50, wt/wt)

Figure 6a provides the current density/voltage characteristics (J/V) of the optimal device obtained from 2-MeTHF. The device shows a short-circuit current (J_{SC}) of 13.2 m A/ cm^2, an open-circuit voltage (V_{OC}) of 0.72 V, and a fill factor (FF) of 54%, corresponding to a PCE of 5.1%. Correspondingly, the best performing device processed from $CHCl_3$ shows the following features: J_{SC} = 12.3 mA/ cm^2, V_{OC} = 0.72 V, FF = 53%, corresponding to a PCE of 4.7%. The external quantum efficiency (EQE) curves of the best performance devices are provided in Figure 6b. As observed, devices show similar quantum efficiencies in the range from 500 to 800 nm, although the device with 2-MeTHF shows slightly higher quantum efficiencies near 450 nm. Both devices show low leakage in current density-voltage characteristics (*J-V)* in the dark, as shown in Figure 7.

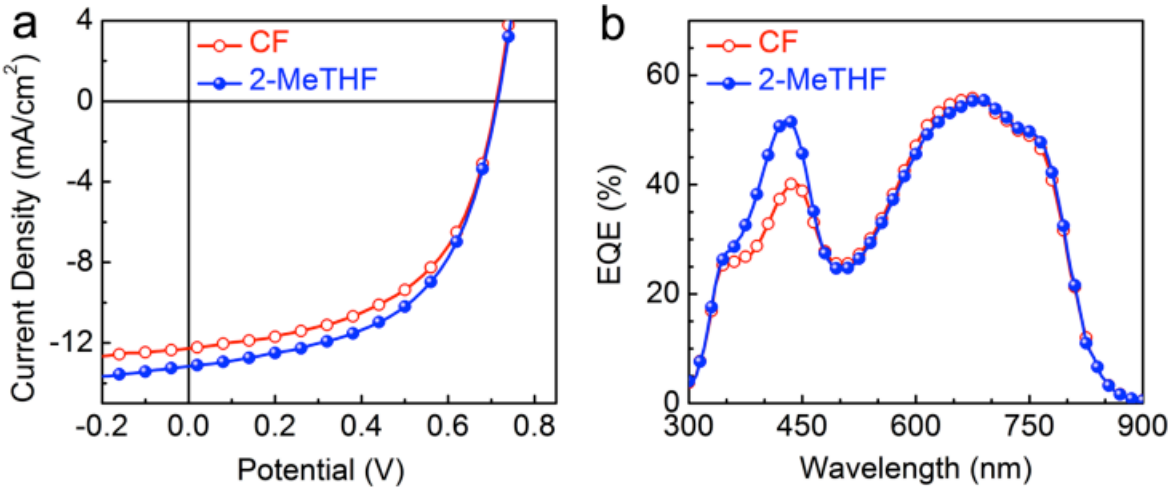

Figure 2-6. (a) *J-V* characteristics, (b) EQE curves of the optimal performance measured from films prepared from 2-MeTHF (spheres) and $CHCl_3$ (circles).

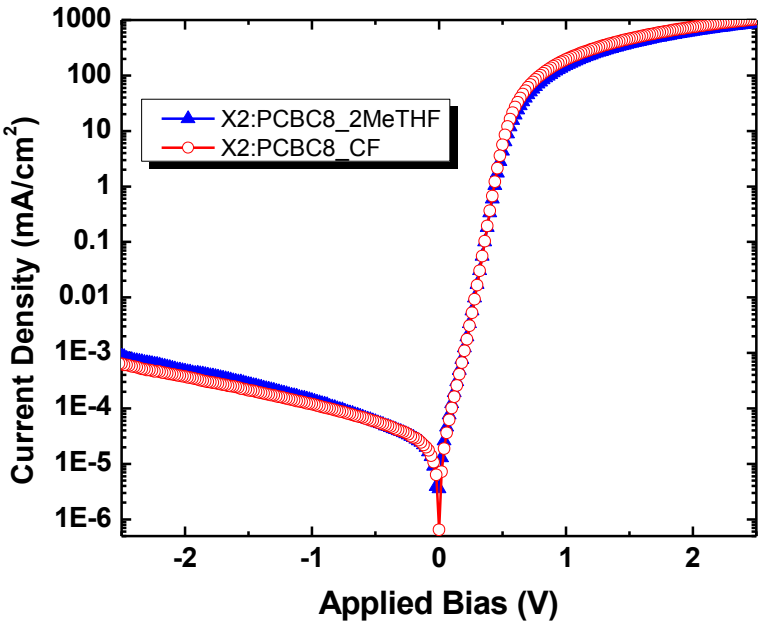

Figure 2-7: The Current density-voltage characteristics (*J-V*) in the dark for best device processed out of $CHCl_3$ (circles) and 2-MeTHF (triangles).

Grazing incidence wide angle X-ray scattering (GIWAXS) data were collected to investigate structural order within the X2 phase in the X2:$PC_{61}BC_8$ blends as a function of solvent used for deposition. [47] Out-of-plane and in-plane reflection profiles are shown in Figures 8 (a) and (b). Films spin-cast from 2-MeTHF or $CHCl_3$ exhibit similar diffraction peaks. These peaks are assigned to π-π stacking (in-plane direction, at q = 1.8 Å^{-1}) and the alkyl chain packing (out-of-plane direction, at q = 0.39 Å^{-1}).[42] Switching from $CHCl_3$ to 2-MeTHF, the crystallite correlation length (CCL) values, which provide an estimation of crystallite size and quality, were calculated using Scherrer equation. In the out-of-plane direction, the CCL values determined using the (100) peak at q = 0.39 Å^{-1} were found to be 11.9 nm ($CHCl_3$) and 12.4 nm (2-MeTHF). Similar analysis for the (010) peak in-plane

direction yields CCL values of 7.5 nm ($CHCl_3$) and 6 nm (2-MeTHF). The similar diffraction profiles and CCL values in the two directions suggest that crystallite features of X2 obtained out of 2-MeTHF and $CHCl_3$ are substantially similar thereby demonstrating the similar ability of the two solvents to organize the BHJ components within the timescale of film formation.

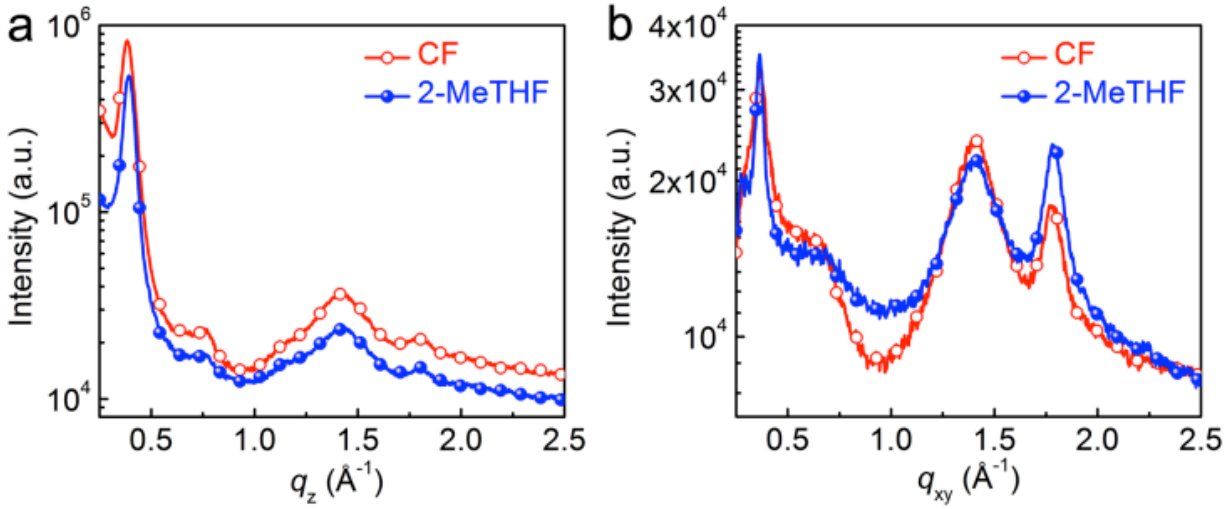

Figure 2-8. Grazing incidence wide angle X-ray scattering (GIWAXS) study of X2:$PC_{61}BC_8$ blend films (25 mg/mL total concentration, D:A= 50:50) prepared from $CHCl_3$ (circles) and 2-MeTHF (spheres): (a) and (b) are ± sector profiles along the nearly out-of-plane and in-plane directions, respectively.

5. Conclusion

In conclusion, we have shown for the first time that molecular solar cells with power conversion efficiencies over 5% can be fabricated by processing X2:$PC_{61}BC_8$ blends from 2-MeTHF. This solvent is derived from agricultural byproducts and is considerably less toxic than widely used aromatic or halogenated alternatives. The donor component, namely X2, was chosen on the basis that BHJ blends with $PC_{61}BM$ were previously demonstrated to

perform well across a wide blend composition range and could function well in the absence of additive or thermal processing protocols. It is worth noting that the X2:$PC_{61}BC_8$ blend provides slightly higher efficiencies from 2-MeTHF relative to the more conventional $CHCl_3$ solvent. Altogether, these findings open new opportunities for considering mass production of organic solar cells, and other optoelectronic devices. It also highlights that substantial molecular design may not be fundamentally necessary for opening environmentally benign processing

6. Experimental Section

Materials and Methods:

Materials: **X2** was synthesized according to the literature.[45] $PC_{61}BM$, $bisPC_{61}BM$ and $PC_{61}BC_8$ were purchased from Solenne BV company. All materials were used as received.

Device fabrication*:* Solar cells devices were fabricated on cleaned, UV/ozone treated Corning 1737 glass patterned with 140 nm ITO. MoO_x films (9 nm) were thermally evaporated on top of ITO substrates at a rate of 0.1 Å/s under vacuum below 10^{-6} torr. The organic films were prepared with different total concentration (20 mg/mL, 25 mg/mL, and 30 mg/mL as indicated in text) with D:A ration of 50:50, wt/wt (also 60:40 for comparison) by spin-coating at 2000 rpm for 60 s. Finally, cathodes were deposited by sequential thermal evaporation of calcium (~10 nm) followed by aluminum (~70 nm) through a shadow mask by thermal evaporation under a vacuum of about 3 x 10^{-7} torr. An aperture with area of 4.5 mm^2 was used during the measurement. Device performances were tested using a Keithly 2602 system Source Meter under illumination by a simulated 100 mW cm^{-2} AM 1.5G light source using a 300 W Xe arc lamp with an AM 1.5 global filter. Solar-simulator irradiance was calibrated using standard silicon photovoltaic with a protective KG1 filter calibrated by the National Renewable Energy Laboratory.

UV-Visible Absorption Spectroscopy*:* optical absorption measurements were performed using a Perkin Elmer Lambda 750 UV-Vis spectrometer. Thin films were prepared by spin-coating on top of MoO_x covered ITO substrates (same condition as device fabrication) at a spin speed of 2000 rpm.

***EQE measurements**:* External quantum efficiencies were determined using a 75 W Xe source, monochromator, optical chopper, lock-in amplifer, and a National Institute of Standards and Technology calibrated silicon photodiode was used for power-density calibration.

***Hole only diode mobility measurements**:* Hole only devices were fabricated on cleaned, UV/ozone treated Corning 1737 glass patterned with 140 nm Indium Tin Oxide. MoO_x was thermally evaporated as a bottom contact at a rate of 0.2 Å/s with a thickness of 10 nm. X2:$PC_{61}BC_8$ was spin cast at 2000 rpm for 60 seconds at a 5:5 blend ratio with a total concentration of 25 mg/mL for both 2-MeTHF and chloroform. A gold top contact was thermally evaporated at 0.2 Å/s with a final thickness of approximately 50 nm. Devices were measured in the dark using a Keithly 2602 system Source Meter.

GIWAXS measurements: GIWAXS patterns were collected at the Stanford Synchrotron Radiation Lightsource (SSRL) beamline 11-3 with an X-ray wavelength of 0.9752 Å, at a 40 cm sample to detector distance at an incident angle of 0.12^o. Samples were probed under a helium environment to minimize beam damage and reduce diffuse scattering. The measurements were calibrated using a LaB6 standard.

7. References

(1) Clark, J. H.; Budarin, V.; Deswarte, F. E. I.; Hardy, J. J. E.; Kerton, F. M.; Hunt, A. J.; Luque, R.; Macquarrie, D. J.; Milkowski, K.; Rodriguez, A.; Samuel, O.; Tavener, S. J.; White, R. J.; Wilson, A. J. *Green Chem*. **2006**, *8*, 853.

(2) Beach, E. S.; Cui, Z.; Anastas, P. T. *Energy Environ. Sci*. **2009**, *2*, 1038.

(3) Sherman, J.; Chin, B.; Huibers, P. D.; Garcia-Valls, R.; Hatton, T. A. *Environ. Health Perspect*. **1998**, *106*, 253.

(4) Guo, X.; Zhang, M.; Cui, C.; Hou, J.; Li, Y. *ACS Appl. Mater. Interfaces* **2014**, *6*, 8190.

(5) Chen, K.-S.; Yip, H.-L.; Schlenker, C. W.; Ginger, D. S.; Jen, A. K.-Y. *Org. Electron*. **2012**, *13*, 2870.

(6) Burke, D. J.; Lipomi, D. J. *Energy Environ. Sci*. **2013**, *6*, 2053.

(7) Burgués-Ceballos, I.; Machui, F.; Min, J.; Ameri, T.; Voigt, M. M.; Luponosov, Y. N.; Ponomarenko, S. A.; Lacharmoise, P. D.; Campoy-Quiles, M.; Brabec, C. J. *Adv. Funct. Mater*. **2014**, *24*, 1449.

(8) Søndergaard, R.; Hösel, M.; Angmo, D.; Larsen-Olsen, T. T.; Krebs, F. C. Mater. *Today* **2012**, *15*, 36.

(9) Cheng, Y.-J.; Yang, S.-H.; Hsu, C.-S. *Chem. Rev*. **2009**, *109*, 5868.

(10) Carsten, B.; He, F.; Son, H. J.; Xu, T.; Yu, L. Chem. Rev. **2011**, *111*, 1493.

(11) Chen, J.; Cao, Y. *Acc. Chem. Res*. **2009**, *42*, 1709.

(12) McCulloch, I.; Ashraf, R. S.; Biniek, L.; Bronstein, H.; Combe, C.; Donaghey, J. E.; James, D. I.; Nielsen, C. B.; Schroeder, B. C.; Zhang, W. *Acc. Chem. Res.* **2012**, *45*, 714.

(13) Blouin, N.; Leclerc, M. *Acc. Chem. Res*. **2008**, *41*, 1110.

(14) Li, Y. *Acc. Chem. Res*. **2012**, *45*, 723.

(15) Moulé, A. J.; Meerholz, K. *Adv. Mater.* **2008**, *20*, 240.

(16) Peet, J.; Kim, J. Y.; Coates, N. E.; Ma, W. L.; Moses, D.; Heeger, A. J.; Bazan, G. C. *Nat. Mater*. **2007**, *6*, 497.

(17) Zalar, P.; Kuik, M.; Ran, N. A.; Love, J. A.; Nguyen, T.-Q. *Adv. Energy Mater*. **2014**, DOI: 10.1002/anem.201400438.

(18) Beaujuge, P. M.; Fréchet, J. M. J. *J. Am. Chem. Soc*. **2011**, *133*, 20009.

(19) Collins, B. A.; Cochran, J. E.; Yan, H.; Gann, E.; Hub, C.; Fink, R.; Wang, C.; Schuettfort, T.; McNeill, C. R.; Chabinyc, M. L.; Ade, H. *Nat. Mater*. **2012**, *11*, 536.

(20) You, J.; Dou, L.; Yoshimura, K.; Kato, T.; Ohya, K.; Moriarty, T.; Emery, K.; Chen, C.-C.; Gao, J.; Li, G.; Yang, Y. *Nat. Commun*. **2013**, *4*, 1446.

(21) Yu, G.; Gao, J.; Hummelen, J. C.; Wudl, F.; Heeger, A. J. *Science* **1995**, *270*, 1789.

(22) Hau, S. K.; Yip, H.-L.; Jen, A. K.-Y. *Polym. Rev*. **2010**, *50*, 474.

(23) Calamari, D.; Galassi, S.; Setti, F.; Vighi, M. *Chemosphere* **1983**, *12*, 253.

(24) Van Hoogen, G.; Opperhuizen, A. *Environ. Toxicol. Chem*. **1988**, *7*, 213.

(25) Heitmuller, P. T.; Hollister, T. A.; Parrish, P. R. Bull. *Environ. Contam. Toxicol.* **1981**, *27*, 596.

(26) http://www.epa.gov/ttn/atw/hlthef/chlorobe.html

(27) Moulé, A. J.; Meerholz, K. *Adv. Funct. Mater*. **2009**, *19*, 3028.

(28) Brabec, C. J.; Gowrisanker, S.; Halls, J. J. M.; Laird, D.; Jia, S.; Williams, S. P. *Adv. Mater*. **2010**, *22*, 3839.

(29) Li, G.; Zhu, R.; Yang, Y. *Nat.* Photonics **2012**, *6*, 153.

(30) Nelson, J. Mater. *Today* **2011**, *14*, 462.

(31) Dang, M. T.; Hirsch, L.; Wantz, G.; Wuest, J. D. *Chem. Rev*. **2013**, *113*, 3734.

(32) Grätzel, M.; Janssen, R. A. J.; Mitzi, D. B.; Sargent, E. H. *Nature* **2012**, *488*, 304.

(33) Chen, Y.; Zhang, S.; Wu, Y.; Hou, *J. Adv. Mater*. **2014**, *26*, 2744.

(34) Duan, C.; Cai, W.; Hsu, B. B. Y.; Zhong, C.; Zhang, K.; Liu, C.; Hu, Z.; Huang, F.; Bazan, G. C.; Heeger, A. J.; Cao, Y. *Energy Environ. Sci*. **2013**, *6*, 3022.

(35) Gu, Y.; Jérôme, F. *Chem. Soc. Rev*. **2013**, *42*, 9550.

(36) Clark, J. H.; Pfaltzgraff, L. A.; Budarin, V. L.; Hunt, A. J.; Gronnow, M.; Matharu, A. S.; Macquarrie, D. J.; Sherwood, J. R. *Pure Appl. Chem*. **2013**, *85*, 1625.

(37) Antonucci, V.; Coleman, J.; Ferry, J. B.; Johnson, N.; Mathe, M.; Scott, J. P.; Xu, J. Org. *Process Res. Dev*. **2011**, *15*, 939.

(38) Pace, V.; Hoyos, P.; Castoldi, L.; Domínguez de María, P.; Alcántara, A. R. *ChemSusChem* **2012**, *5*, 1369.

(39) Shanmuganathan, S.; Natalia, D.; van den Wittenboer, A.; Kohlmann, C.; Greiner, L.; Domínguez de María, P. *Green Chem*. **2010**, *12*, 2240.

(40) Simeó, Y.; Sinisterra, J. V.; Alcántara, A. R. Green Chem. 2009, 11, 855.

(41) Liu, X.; Sun, Y.; Perez, L. A.; Wen, W.; Toney, M. F.; Heeger, A. J.; Bazan, G. C. *J. Am. Chem. Soc.* **2012**, *134*, 20609.

(42) Huang, Y.; Liu, X.; Wang, C.; Rogers, J. T.; Su, G. M.; Chabinyc, M. L.; Kramer, E. J.; Bazan, G. C. *Adv. Energy Mater*. **2014**, DOI: 10.1002/anem.201301886.

(43) Zhang, Y.; Blom, P. W. M. *Appl. Phys. Lett*. **2011**, *98*, 143504.

(44) Nicolai, H. T.; Wetzelaer, G. a. H.; Kuik, M.; Kronemeijer, A. J.; Boer, B. de; Blom, P. W. M. *Appl. Phys. Lett*. **2010**, *96*, 172107.

(45) Rose, A. *Phys. Rev.* **1955**, *97*, 1538

(46) Mandoc, M. M.; Koster, L. J. A.; Blom, P. W. M. *Applied Physics Letters* **2007**, *90*, 133504.

(47) Rivnay, J.; Mannsfeld, S. C. B.; Miller, C. E.; Salleo, A.; Toney, M. F. *Chem. Rev*. **2012**, *112*, 5488.